Ge-doped silica nanoparticles: production and characterisation

A. Alessi,[1,*] M. Fanetti,[2] S. Agnello,[3] S. Girard,[1] G. Buscarino,[3] D. Di Francesca,[1] I. Reghioua,[1] F. Messina,[3] M. Cannas,[3] L. Martin-Samos,[2] M. Valant,[2] N. Richard,[4] A. Boukenter,[1] and Y. Ouerdane[1]

[1]*Univ-Lyon, Laboratoire H. Curien, UMR CNRS 5516, 18 rue du Pr. Benoît Lauras 42000, Saint-Etienne, France*
[2]*Materials Research Laboratory, University of Nova Gorica, Vipavska 11c 5270-Ajdovscina, Slovenia*
[3]*Dipartimento di Fisica e Chimica, Università di Palermo, I-90123 Palermo, Italy*
[4]*CEA, DAM, DIF, F-91297 Arpajon, France*
[*]*Antonino.alessi@univ-st-etienne.fr*

Abstract: Silica nanoparticles were produced from germanosilicate glasses by KrF laser irradiation. The samples were investigated by cathodoluminescence and scanning electron microscopy, providing the presence of nanoparticles with size from tens up to hundreds of nanometers. The emission of the Germanium lone pair center is preserved in the nanoparticles and atomic force microscopy revealed the presence of no spherical particles with a size smaller than ~4 nm. The absorption coefficient enhancement induced by Ge doping is reputed fundamental to facilitate the nanoparticles production. This procedure can be applied to other co-doped silica materials to tune the nanoparticles features.

OCIS codes: (160.4236) Nanomaterials; (160.6030) Silica; (160.4670) Optical materials.

References and links

1. S. Logothetidis, *Nanostructured Materials and Their Applications* (Springer-Verlag, 2012).
2. M. De, P. S. Ghosh, and V. M. Rotello, "Applications of nanoparticles in biology," Adv. Mater. **20**(22), 4225–4241 (2008).
3. D. Knopp, D. Tang, and R. Niessner, "Review: bioanalytical applications of biomolecule-functionalized nanometer-sized doped silica particles," Anal. Chim. Acta **647**(1), 14–30 (2009).
4. L. Wang, K. Wang, S. Santra, X. Zhao, L. R. Hilliard, J. E. Smith, Y. Wu, and W. Tan, "Watching silica nanoparticles glow in the biological world," Anal. Chem. **78**(3), 646–654 (2006).
5. D. Lin, W. Liu, Y. Liu, H. R. Lee, P.-C. Hsu, K. Liu, and Y. Cui, "High ionic conductivity of composite solid polymer electrolyte via in situ synthesis of monodispersed SiO_2 nanospheres in poly(ethylene oxide)," Nano Lett. **16**(1), 459–465 (2016).
6. M. A. Noginov, G. Zhu, A. M. Belgrave, R. Bakker, V. M. Shalaev, E. E. Narimanov, S. Stout, E. Herz, T. Suteewong, and U. Wiesner, "Demonstration of a spaser-based nanolaser," Nature **460**(7259), 1110–1112 (2009).
7. L. M. Liz-Marzán, M. Giersig, and P. Mulvaney, "Synthesis of nanosized gold–silica core–shell particles," Langmuir **12**(18), 4329–4335 (1996).
8. T.-F. Tseng and J.-Y. Wu, "Preparation and structural characterization of novel nanohybrids by cationic 3D Silica nanoparticles sandwiched between 2D anionic montmorillonite clay through electrostatic attraction," J. Phys. Chem. C **113**(30), 13036–13044 (2009).
9. W. L. Zhang and H. J. Choi, "Silica-graphene oxide hybrid composite particles and their electroresponsive characteristics," Langmuir **28**(17), 7055–7062 (2012).
10. D. Arcos and M. Vallet-Regí, "Bioceramics for drug delivery," Acta Mater. **61**(3), 890–911 (2013).
11. H. Chen, G. D. Wang, Y.-J. Chuang, Z. Zhen, X. Chen, P. Biddinger, Z. Hao, F. Liu, B. Shen, Z. Pan, and J. Xie, "Nanoscintillator-mediated X-ray inducible photodynamic therapy for in vivo cancer treatment," Nano Lett. **15**(4), 2249–2256 (2015).
12. X. Liu, D. Du, and G. Mourou, "Laser ablation and micromachining with ultrashort laser pulses," IEEE J. Quantum Electron. **33**(10), 1706–1716 (1997).
13. S. I. Dolgaev, A. V. Simakin, V. V. Voronov, G. A. Shafeev, and F. Bozon-Verduraz, "Nanoparticles produced by laser ablation of solids in liquid environment," Appl. Surf. Sci. **186**(1-4), 546–551 (2002).
14. J. Ihlemann, B. Wolff, and P. Simon, "Nanosecond and femtosecond excimer laser ablation of fused silica," Appl. Phys., A Mater. Sci. Process. **54**(4), 363–368 (1992).
15. J. H. Brannon, "Micropatterning of surfaces by excimer laser projection," J. Vac. Sci. Technol. B **7**(5), 1064–1071 (1989).
16. P. Schaaf, *Laser Processing of Materials Fundamentals, Applications and Developments* (Springer, 2010).

#264567 Received 9 May 2016; revised 30 May 2016; accepted 30 May 2016; published 9 Jun 2016

17. M. Bass, *Laser Materials Processing* (North-Holland Publishing Company, 1983).
18. D. Du, X. Liu, G. Korn, J. Squier, and G. Mourou, "Laser-induced breakdown by impact ionization in SiO2 with pulse widths from 7 ns to 150 fs," Appl. Phys. Lett. **64**(23), 3071 (1994).
19. D. Von der Linde and H. Schüler, "Breakdown threshold and plasma formation in femtosecond laser–solid interaction," J. Opt. Soc. Am. B **13**(1), 216–222 (1996).
20. B. C. Stuart, M. D. Feit, S. Herman, A. M. Rubenchik, B. W. Shore, and M. D. Perry, "Nanosecond-to-femtosecond laser-induced breakdown in dielectrics," Phys. Rev. B Condens. Matter **53**(4), 1749–1761 (1996).
21. L. Skuja, "Isoelectronic series of twofold coordinated Si, Ge, and Sn atoms in glassy SiO_2: a luminescence study," J. Non-Cryst. Solids **149**(1-2), 77–95 (1992).
22. K. Awazu, H. Kawazoe, and M. Yamane, "Simultaneous generation of optical absorption bands at 5.14 and 0.452 eV in 9 SiO_2:GeO_2 glasses heated under an H_2 atmosphere," J. Appl. Phys. **68**(6), 2713–2718 (1990).
23. A. Alessi, S. Agnello, Y. Ouerdane, and F. M. Gelardi, "Dependence of the emission properties of the germanium lone pair center on Ge doping of silica," J. Phys. Condens. Matter **23**(1), 015903 (2011).
24. A. Alessi, S. Girard, M. Cannas, S. Agnello, A. Boukenter, and Y. Ouerdane, "Evolution of photo-induced defects in Ge-doped fiber/preform: influence of the drawing," Opt. Express **19**(12), 11680–11690 (2011).
25. A. Alessi, S. Girard, I. Reghioua, M. Fanetti, D. Di Francesca, S. Agnello, M. Cannas, C. Marcandella, L. Martin-Samos, N. Richard, A. Boukenter, and Y. Ouerdane, "Gamma and x-ray irradiation effects on different Ge and Ge/F doped optical fibers," J. Appl. Phys. **118**(8), 085901 (2015).
26. D. L. Griscom, "On the natures of radiation-induced point defects in GeO_2-SiO_2 glasses: reevaluation of a 26-year-old ESR and optical data set," Opt. Mater. Express **1**(3), 400–412 (2011).
27. K. T. V. Grattan and B. T. Meggitt, *Optical Fiber Sensors Technology, Advanced Application, Bragg Gratings and Distributed Sensors* (Kluwer Academic Publishers, 2000).
28. M. Essid, J. Albert, J. L. Brebner, and K. Awazu, "Correlation between oxygen-deficient center concentration and KrF excimer laser induced defects in thermally annealed Ge-doped optical fiber preforms," J. Non-Cryst. Solids **246**(1-2), 39–45 (1999).
29. M. Takahashi, T. Uchino, and T. Yoko, "Correlation between Macro- and Microstructural Changes in Ge:SiO_2 and SiO_2 Glasses under Intense Ultraviolet Irradiation," J. Am. Ceram. Soc. **85**(5), 1089–1092 (2002).
30. N. Richard, S. Girard, L. Giacomazzi, L. Martin-Samos, D. Di Francesca, C. Marcandella, A. Alessi, P. Paillet, S. Agnello, A. Boukenter, Y. Ouerdane, M. Cannas, and R. Boscaino, "Coupled theoretical and experimental studies for the radiation hardening of silica-based optical fibers," IEEE Trans. Nucl. Sci. **61**(4), 1819–1825 (2014).
31. M. Nakamura, M. Shono, and K. Ishimura, "Synthesis, characterization, and biological applications of multifluorescent silica nanoparticles," Anal. Chem. **79**(17), 6507–6514 (2007).
32. P. Teolato, E. Rampazzo, M. Arduini, F. Mancin, P. Tecilla, and U. Tonellato, "Silica nanoparticles for fluorescence sensing of Zn(II): exploring the covalent strategy," Chemistry **13**(8), 2238–2245 (2007).
33. E. Vella and R. Boscaino, "Structural disorder and silanol groups content in amorphous SiO_2," Phys. Rev. B **79**(8), 085204 (2009).
34. F. Messina, M. Cannas, and R. Boscaino, "Generation of defects in amorphous SiO_2 assisted by two-step absorption on impurity sites," J. Phys. Condens. Matter **20**(27), 275210 (2008).
35. A. Alessi, G. Iovino, G. Buscarino, S. Agnello, and F. M. Gelardi, "Entrapping of O_2 molecules in nanostructured silica probed by photoluminescence," J. Phys. Chem. C **117**(6), 2616–2622 (2013).

1. Introduction

Nanotechnology is a large interdisciplinary domain of material science research involving physic, chemistry, biology, medicine, sustainable development. The great interest in nanomaterials is related to the desire of considerably decrease the size of optical and electronic devices and in view of peculiar properties of the nano-sized materials with respect to their bulk counterpart [1]. A fundamental reason of interest to study and to produce nanoparticles is constituted by their applications in biosensing, drug and biomolecular delivery and bioimaging [2], applications which are strictly related to medical field. Nano-silica systems were employed in such biological fields [3,4] but also in other cases such as production of solid polymer electrolyte [5], nanolaser [6] and various nanocomposite systems [7–11]. The use of lasers to process materials is a diffused technique [12–17]. As reported [12,14] material removal during ablation is a consequence of the high energy absorption of the materials from the laser source. This phenomenon can take place even if the absorption coefficient at the laser wavelength is low and it can be enhanced by adding dopants [14]. The absorption of light from the target can be due to linear or nonlinear processes [12], whereby the energy absorption mechanisms depend on the material optical properties and on the features (wavelength, duration, power…) of the employed laser pulse. Linear absorption is dominant for opaque materials especially for low intensity and/or pulses of relatively long durations (ns or longer), whereas the nonlinear processes are responsible for the absorption in transparent (at the wavelength of the laser) materials, which generates the laser-induced

#264567 Received 9 May 2016; revised 30 May 2016; accepted 30 May 2016; published 9 Jun 2016

optical break-down. Such nonlinear processes are usually observed for ultrashort (sub-picosecond) laser pulses having high intensity [12].

Laser ablation of pure silica was studied employing different wavelengths and pulse durations (from tens of nanoseconds down to hundreds of femtoseconds) [14], but this investigation was focused on the modifications induced at surface, without testing the possibility to generate nanoparticles. Laser-induced break-down of silica was also investigated in [18,19], evidencing the dependence on the laser pulse duration and, the need of high intensity to observe it on the target surface. In [20] Stuart et al. reported an experimental and theoretical investigation on the laser-induced break-down considering pulse widths ranging from the nanosecond to the femtosecond. This investigation indicates that very short and intense pulses induce multiphoton ionization. The measured damage was attributed to melting, boiling or fracture of the sample surface for laser pulses longer than 50 ps, and to ablation for those with duration shorter than 10 ps. In these cases the production of nanoparticles from the target was not investigated. As above mentioned, the presence of dopant can increase the optical absorption of the materials and this can be employed to facilitate the material removal of from the target. The presence of defects or impurities can play a significant role in the material's response when submitted to lengthy duration laser pulses since they can provide electrons [12,20] acting as starting "seed" electrons for avalanche ionization [12].

Some relevant aspects regarding Ge-doped silica need to be highlighted. First of all, the Ge atoms are linked, as substitutional atoms, to the silica matrix, rather than being hosted as interstitial atoms. Then, Ge doping usually introduces Ge related defects called GLPC (Germanium lone pair center), having an absorption band ~5.1 eV (~240 nm) [21–23] and emission at ~3.2 eV (~390 nm) and ~4.3 eV (290 nm). This defect is considered as one of the main causes of the photosensitivity of the Ge doped silica under both ionizing and laser irradiations [24–26]. This process is used for the photo-inscription of Fiber Bragg grating [27–29] into waveguides and it can induce significant matrix modification [29]. Then, it should be reminded that the Ge-doped silica used for the drawing of optical fibers are typically rich of GLPC [24] and that the Ge doping decreases the silica band gap [30]. All these features are of particular concern for the application of Ge-doped silica for nanoparticles production by laser ablation. Notwithstanding, few works considered these potentialities.

In this manuscript we report evidences of the production of Ge-doped silica nanoparticles from standard glasses. These glasses were irradiated with a KrF laser while they were immersed in distilled water. The samples were characterized by SEM, AFM, EDX and cathodoluminescence techniques. Although the production process will still be improved to avoid the micro-particles formation and to achieve a better control of the nanoparticles sizes, it represents an innovative, quite easy production technique of emitting nanoparticles.

2. Experimental

We employed two different Ge-doped silica glasses. They were manufactured by standard procedures used for the production of optical fibers preforms. The sample named Ge20 was obtained by Plasma-activated Chemical Vapor Deposition (PCVD). It contains a Ge doping level of 20 weight percent (wt%). The sample named Ge8 contains a maximum Ge doping level of 8 wt%. It was obtained by using the MCVD (modified chemical vapor deposition) process. The two samples were immersed in distilled water when exposed to the focused (spot size ~1 mm) 248 nm light of a KrF pulsed (pulse duration 30 ns, repetition 10 Hz) laser (COMPex 110 from Lambda Physik), having an energy of 140 mJ per pulse.

The samples were moved after few laser pulses along the plan orthogonal to the laser beam and the laser focus along the vertical was also adjusted. This procedure was applied to keep the laser beam focused on the surfaces. In fact, few pulses were efficient to destroy the samples in the irradiated region or to remove a relevant amount of material.

Scanning electron microscopy images of the powders obtained after the evaporation of the water and their deposition on a carbon tape substrate were acquired with field-emission SEM

#264567 Received 9 May 2016; revised 30 May 2016; accepted 30 May 2016; published 9 Jun 2016

(JSM 7100F, JEOL) with electron energy of 15 keV and current 10-15 nA. No conductive coating was applied on the samples. The same apparatus is equipped with EDX (energy dispersive X-ray spectroscopy) detector (X-Max 80 OXFORD) and with a cathodoluminescence (CL) spectroscopy and mapping apparatus (MONOCL4, GATAN) working in the spectral range 300-750 nm (1.7 - 4 eV), which were employed to perform CL and EDX measurements.

EDX, CL image and spectra were acquired with a probe current of 10-15 nA and electron energy of 15 keV. In the employed experimental conditions, the particle substrate (carbon tape) does not emit a detectable CL signal in the investigated spectral domain.

Atomic Force Microscopy (AFM) measurements were done in air by a Bruker FAST-SCAN microscope working in soft tapping mode and using a FAST-SCAN-A probe (27 μm long triangular Silicon Nitride cantilever) with the following characteristics: 1400 kHz resonant frequency, 17 N/m force constant and about 5 nm apical radius. For AFM image, to facilitate the detection of isolated small particles, the powder samples were further diluted in distilled water and some drops of the solution were allowed to dry on a mica substrate.

VUV absorption spectra were acquired with an ACTON single-beam spectrophotometer (mod.SP150), working in N_2 flux, equipped with a D2 lamp (30 W) and with two identical monochromators (1200 lines/mm). Measurements were performed with a bandwidth of 0.5 nm. All the measurements were performed at room temperature.

3. Result

In Fig. 1(a) we report the SEM image recorded on the nano-powder produced from Ge8 sample. In this image we observe the presence of big particles, having sizes of hundreds of nanometers, and the presence of different groups of smaller particles, having size of ten or few tens of nanometers. To better characterize these nanoparticles, we recorded CL images, CL and EDX measurements. These data are reported in the Figs. 1(b), 1(c) and 1(d), respectively. By comparing CL image and SEM image we observe a strict correspondence between the presence of CL signal and the morphological characteristic observed by the SEM. We detected not only very large particles or groups of particles, but also small groups of particles, as it can be seen from the central and the superior part of the zone highlighted by the red square of Fig. 1(b). The origin of this emission is clarified by the spectrum (recorded in the central part of the red square of Fig. 1(b)) reported in Fig. 1(c), in which the presence of an emission band at ~400 nm is clear. This band is a well-known emission band and it is attributed to the GLPC (structural model reported in Fig. 1(c)) [21–23].

Figure 1(d) illustrates the EDX image obtained by monitoring the signal of the Si line. The image was acquired in the same region of the red square pictured in Fig. 1(b). In this image we clearly recognize the main features previously detected in SEM and CL images. In the upper and in the central part of Fig. 1(d) small groups of nanoparticles are detected even if the signal only slightly overcomes the detection limit. As a consequence of the small particles size and the doping level, the amount of Ge was not high enough to allow to perform an EDX map comparable to those obtained for the Si signal.

In Fig. 2 we report the SEM and CL images (Figs. 2(a) and 2(b), respectively) recorded for the powder of the Ge20 sample. As for the previous sample we observe a relevant correspondence between the morphological and the CL images. These images illustrate the presence of several agglomerates/aggregates of nanoparticles with sizes of tens and hundreds of nanometers. Furthermore, the CL signal (reported in Fig. 2(c) together with the zoom of the region where the signal was acquired) consists of a peak at ~410 nm and a shoulder at higher wavelengths. This latter can be attributed to the ~460 nm (2.7 eV) emission of the ODC(II). This defect consists in a twofold coordinated Si having an electron lone pair [21]. The 410 nm peak can be attributed to the GLPC and the shift of the maximum could be due to the overlap with the emission at higher wavelengths, or to a slight charging of the sample during the spectrum acquisition. In this case, the low amplitude of the ODC(II) emission and the overlap with the GLPC activity prevent the precise estimation of its peak and the detection of possible shifts.

#264567 Received 9 May 2016; revised 30 May 2016; accepted 30 May 2016; published 9 Jun 2016

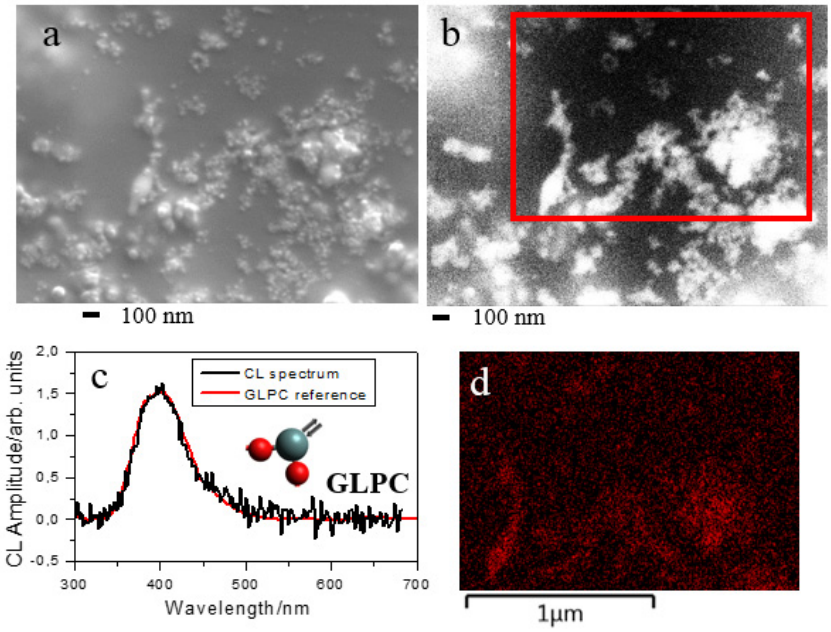

Fig. 1. a) SEM image (~2.4 × 1.8 µm) of the Ge8powder; b) panchromatic CL image (~2.4 × 1.8 µm) of the same zone illustrated in panel a, the red square highlights the region were we performed the Si signal EDX image of panel d; c) (—) CL spectrum acquired in the center of the red square of panel b and (—) GLPC spectrum recorded in a Ge doped optical fiber; d) Si EDX map acquired in the area marked in red in b).

In Fig. 2(d) we report the SEM image of agglomerates/aggregates and of particles. The inset in the upper part of the figure illustrates the Si signal EDX image, whereas the other inset illustrates the EDX image of the Ge signal. As for the previous sample, in the Si EDX image we recognize the signal originating from agglomerates/aggregates and particles with sizes some hundreds of nanometers or larger. The Ge signal, by contrast, is still hardly detectable and it seems to be above the noise threshold only in the central part of the image.

To investigate the presence of small nanoparticles, we acquired AFM images. In both samples we detected the presence of some isolated nanoparticles. Some of the data recorded for both samples are reported in Fig. 3(a) and 3(b) illustrate the image recorded for the sample Ge8 and Ge20 respectively. By evaluating the size of the particles in the xy plane and in the vertical direction we noted that these nanoparticles are not spherical, having a vertical size of few nanometers but at least one size in the xy plane of the order of few tens of nanometers.

#264567 Received 9 May 2016; revised 30 May 2016; accepted 30 May 2016; published 9 Jun 2016

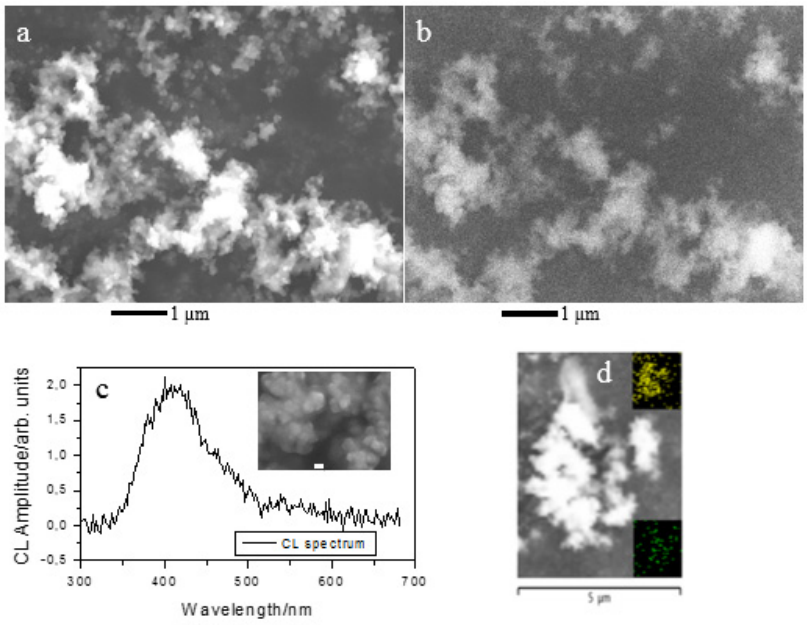

Fig. 2. a) SEM image (~6.9 × 5.2 µm) of the Ge20 powder; b) panchromatic CL image (~7 × 5.2 µm) of the same; c) CL spectrum of the Ge20 sample and SEM image of the zone (~1.8 × 1.3 µm) where the spectrum was recorded (scale bar 100 nm); d) SEM image of the Ge20 powder showing a cluster of nanoparticles, with EDX map of the Si signal (top inset) and of the Ge signal (bottom inset) acquired on the same cluster.

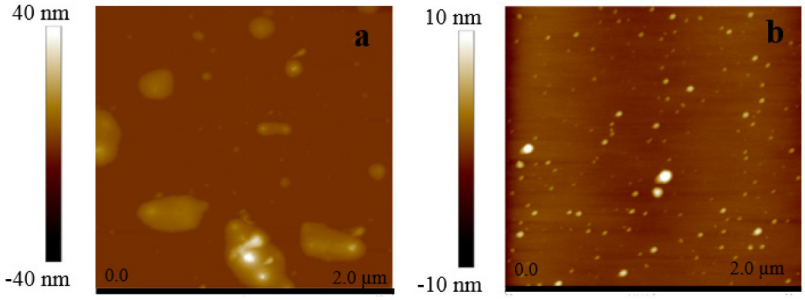

Fig. 3. AFM images recorded for the powder obtained by the KrF laser irradiation of the Ge8 glass (panel a) and Ge20 (panel b).

4. Discussion

All these data clearly indicate the production of luminescent Ge doped particles and nanoparticles from the starting glass. On the one hand, the presence of micro-particles should be avoided since it implies that a relevant mass of the samples is not employed for the nanoparticles production. On the other hand, the presence of particles with sizes of hundreds of nanometers is not necessarily a disadvantage. In fact, for some biological applications nanoparticles of 500/300 nm [31], and from ten to hundreds nm [3,4] (up to 600 nm [32]) were previously proposed or employed. Further control on the size of the obtained nanoparticles could be achieved by changing the laser wavelength, duration, photon flux or fluence.

Regarding the employed starting samples we note that the G8 glass has a high GLPC content as the one reported for similar samples in [24]. By contrast, in the Ge20 glass the

#264567 Received 9 May 2016; revised 30 May 2016; accepted 30 May 2016; published 9 Jun 2016

GLPC content is lower, but the higher Ge content implies larger decrease of the band gap. In Fig. 4, we report the OA (optical absorption) spectrum recorded for this sample up to the VUV spectral domain. Such spectrum clearly shows a high absorption coefficient and a significant difference with the one detected in OH- and defect-free pure-silica materials [33].

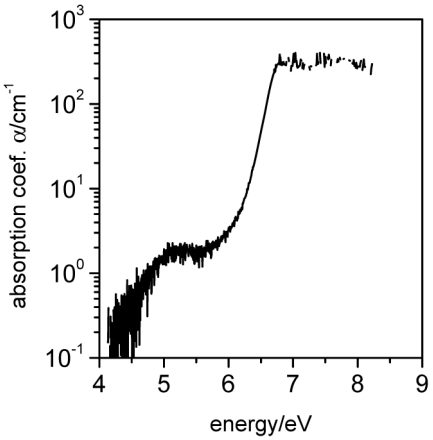

Fig. 4. Optical absorption spectrum recorded for a Ge20 sample having a thickness of 0.3 mm.

These two considerations prove that the incorporation of Ge atoms into silica provides a relevant increase of the absorption coefficient in the UV and VUV spectral domain, improving the energy absorption by the target. Indeed, the multi-photons processes needed for multi-photons ionization require a lower number of photons with respect to that needed in pure silica and obviously the defects contribute with their optical absorption to transfer the laser energy to the glass network. All these factors can help avalanche and multi-photons ionization. The high sensitivity of the Ge doped materials to the UV laser was reported [29] and it results not only into point defects generation but also into some matrix reorganization. Then, silica related defects can be generated by two-steps processes by irradiation with a 5 ns pulsed laser at ~5.1 eV (243 nm) [34]. We underline that the 243 nm is in the spectral range of the GLPC optical absorption, as the here employed laser. So the results obtained in [34] support the idea that multi-photons processes can be induced in Ge-doped materials using this typology of lasers. Considering previous investigations [12] and the long time duration of our laser pulse we expect that the absorbed energy is transferred to a sample volume larger than the one in which the laser is focused and that the material is mainly removed after the heating of the samples. Anyway, it seems difficult that micro-particles are generated after melting or/and vaporization. So their presence could be related to the fact that in different moments of the irradiation the samples featured some explosions, generated by the induced thermal gradient, as-made stress or inhomogeneities in the samples. Anyway, the present investigation proves the possibility to produce luminescent Ge-doped silica nanoparticles. We underline that the Ge doping can be used to obtain silica nanoparticles intrinsically luminescent and that they can be further adapted to specific applications applying surface functionalization processes [4] or through loading with O_2 [35].

Furthermore, employing samples containing other luminescent codopants, already used in optical fiber technology, nanoparticles with specific properties can be produced too. We highlight that there are not evidences that the dopant could come out from the network, whereas the leak of dye trapped in the nanoparticles can take place [4].

5. Conclusion

We produced silica nanoparticles starting from standard Ge-doped glasses already employed in other technological fields. By immerging these glasses in water during the irradiation with a KrF laser we obtained emitting nanoparticles. These particles were characterized in sizes by

#264567 Received 9 May 2016; revised 30 May 2016; accepted 30 May 2016; published 9 Jun 2016

SEM and AFM. The first technique coupled with cathodoluminescence mapping provide evidence for the presence of nanoparticles with sizes of tens and of hundreds of nanometers and of different agglomerate/aggregates. Such results were supported by EDX analysis of the samples. AFM images evidenced the presence and to characterize the sizes of isolated non spherical nanoparticles. The role of the Ge doping in facilitating the energy absorption of the target from the laser is also discussed and VUV data are supporting this aim. Even though the presented procedure is still under improvement to avoid the presence of micro-particles, it proves the possibility to obtain emitting silica nanoparticles, which can be further tuned in properties applying already known procedures in literature. Finally, we note that by considering starting silica samples containing also other emitting codopants, a larger tunability of nanomaterials will be achieved.

#264567 Received 9 May 2016; revised 30 May 2016; accepted 30 May 2016; published 9 Jun 2016